



Potter, J. N., Wilcox, P. D., & Croxford, A. J. (2018). Diffuse field full matrix capture for near surface ultrasonic imaging. *Ultrasonics*, 82, 44-48. <https://doi.org/10.1016/j.ultras.2017.07.009>

Peer reviewed version

License (if available):  
CC BY-NC-ND

Link to published version (if available):  
[10.1016/j.ultras.2017.07.009](https://doi.org/10.1016/j.ultras.2017.07.009)

[Link to publication record in Explore Bristol Research](#)  
PDF-document

This is the author accepted manuscript (AAM). The final published version (version of record) is available online via Elsevier at <http://www.sciencedirect.com/science/article/pii/S0041624X1730197X> . Please refer to any applicable terms of use of the publisher.

## University of Bristol - Explore Bristol Research

### General rights

This document is made available in accordance with publisher policies. Please cite only the published version using the reference above. Full terms of use are available:  
<http://www.bristol.ac.uk/pure/about/ebr-terms>

# Diffuse field full matrix capture for near surface ultrasonic imaging

J. N. Potter<sup>1</sup>, P. D. Wilcox and A. J. Croxford

*Department of Mechanical Engineering  
University of Bristol  
Bristol, UK*

---

## Abstract

This article reports a technique for near-surface ultrasonic array imaging. Information equivalent to an undelayed full matrix of inter-element responses is produced through cross-correlation of a later time diffuse full matrix. This reconstructed full matrix lacks the nonlinear effects of early time saturation present in a directly acquired response. Consequently the near-surface material information usually obscured by this effect is retrieved. Furthermore it is shown that a hybrid full matrix formed through a temporally weighted sum of coherent and reconstructed matrices allows for effective near-surface and bulk material imaging from a single direct-contact experimental realisation.

*Keywords:* Ultrasonics, imaging, diffuse fields, Green's functions

---

## 1. Introduction

The response of an ultrasonic transducer in pulse-echo operation contains nonlinear effects caused by physical limitations of acquisition systems which obscure early time acoustic information. This response is characterised firstly by the finite time associated with the switch from transmission to reception operation, combined with the saturation from remnants of the initial activation (e.g. ultrasonic reverberation within the transducer) and nonlinear electronic recovery process. This problem is compounded when using ultrasonic arrays for which the close proximity of elements leads to saturation

---

<sup>1</sup>e-mail: jack.potter@bristol.ac.uk

of neighbouring elements through electrical and mechanical cross-talk. The consequence of this is to effectively blind an ultrasonic inspection system to the area immediately in front of the array. In common engineering materials this blind region can extend to several mm and is therefore not insignificant.

This may be mitigated in part through the introduction of a stand-off medium (sometimes referred to as a delay line) between the transducer and specimen. This has undesirable effects, namely a reduction in acoustic energy transmitted to the specimen and the potential introduction of additional refracted modes which may induce imaging artefacts. Furthermore this is not always possible in applications which require low-profile, embedded or permanently bonded transducers. Access to early time responses also opens up potential applications for super-resolution imaging as it may allow evanescent fields local to sub-wavelength scatterers to be interrogated directly. Consequently, it is desirable to remove the effects of saturation and element cross-talk without requiring a stand-off medium. The approach proposed here is to recover near surface information through cross-correlation of diffuse fields.

Some sufficient time after transmission of sound into a bounded system, through the effects of multiple scattering, the field will appear to homogenise to a diffuse-like state. Although statistically the field may be considered uniform (neglecting weak localisation effects [1]), spatial phase correlations persist within a diffuse field. It has previously been shown[9, 10] that ensemble averaging the cross-correlation of response at two points within a diffuse field will reproduce the heterogeneous Green's function between the two points. Practically the ensemble average may be approximated through multiple excitations at different source locations or cross-correlation of different temporal windows.

This has found application particularly in the fields of seismology and geo-physics[7, 3, 8, 5, 2, 11]. By cross-correlating the coda of seismic events recorded at monitoring stations, the direct response between the stations is obtained. Through this, a virtual array of emitters and receivers is formed. The recovery of Green's functions from diffuse fields has generally been considered of little relevance for non-destructive testing applications since if sound can be recorded at a point then it is trivial to also transmit sound at the same point, thereby allowing direct responses to be obtained explicitly. Where the process is of use is in revealing information obscured by the operating limitations of the acquisition systems.

The nonlinear effects that obscure early time information in ultrasonic measurements are only present within a directly acquired signal. Whereas

near-surface information is only present within the obscured region of a direct acquisition, it is implicitly contained throughout the diffuse field and may be retrieved through cross-correlation. It is shown here that signals equivalent to an undelayed full matrix of ultrasonic array data can be recovered from the diffuse field. Crucially this omits effects of early time saturation, allowing for near-surface imaging to be achieved from direct contact measurements.

## 2. Full matrix reconstruction

Full matrix capture is the process of sequential acquisition of responses for each transmitter-receiver element pair of an ultrasonic array which are then collated to form the so-called full matrix [4]. Typically, phase delays are then applied in post-processing, under an assumption of linear superposition, to emulate the interference effects of equivalent physical beam forming. Through this, sophisticated imaging may be achieved without the prohibitively long acquisition time which would be required with parallel element transmission. Here the time domain responses of the full matrix shall be denoted  $h_{i,j}(t)$ , where the first and second indices correspond to transmitting and receiving elements respectively. Specifically  $h_{i,j}(t)$  shall be reserved for a conventional coherent full matrix in which time zero of the recorded window coincides with the transmission time. The diffuse full matrix, obtained by initiating recording some sufficiently long time,  $t_r$ , after transmission, has previously been used in this form for nonlinear ultrasonic imaging [6]. Although it may be considered to simply be a later window of the matrix  $h_{i,j}(t)$ , here we will denote the diffuse full matrix  $d_{i,j}(t)$  in order to make the distinction clear. If both have a window length of  $T$ , the spectra of the coherent and diffuse full matrices are  $H_{i,j}(\omega) = \int_0^T h_{i,j}(t)e^{i\omega t} dt$  and  $D_{i,j}(\omega) = \int_{t_r}^{t_r+T} d_{i,j}(t)e^{i\omega t} dt$  respectively.

The aim here is to process the diffuse full matrix  $d_{i,j}(t)$  in a such a way as to obtain a matrix equivalent to  $h_{i,j}(t)$  but that is not polluted by the non-linear measurement artefacts that obscure early time data. In order for the Green's functions to effectively emerge through cross-correlation, a practical approximation must be made to the theoretical ensemble average. Since the full matrix contains responses for the individual transmissions of each element, source averaging can be exploited to obtain the necessary phase perturbations to the field.

A reconstructed full matrix,  $g_{i,j}$ , is obtained by cross-correlating the responses of element  $i$  with that of element  $j$ , averaged over all transmitting

elements. For an  $N$  element array, in the time domain this may be written as follows

$$h_{i,j}(t) \approx g_{i,j}(\tau) = \frac{1}{N} \sum_{k=1}^N \int_{t_r}^{t_r+T} d_{k,i}(t) d_{k,j}(t + \tau) dt. \quad (1)$$

Equivalently, in the frequency domain this is simply the inner product of each element response spectra and the conjugate of the other, again averaged over transmissions as follows

$$G_{i,j}(\omega) = \frac{1}{N} \sum_{k=1}^N D_{k,i}(\omega) \bar{D}_{k,j}(\omega). \quad (2)$$

In practice the cross-correlation need only be performed over the bandwidth required for subsequent imaging. What is obtained is an approximation to the inter-element Green's functions convolved with the element transfer functions. This may be regarded as a time reversal operation in that, through processing, the later time diffuse full matrix is transformed to the equivalent matrix with no reception delay.

### 3. Near surface imaging

Full matrix reconstruction was applied to the inspection of a rectilinear aluminium block with artificial near-surface defects. The block had dimensions of 30x50x20mm and the defects were a series of 0.5 mm diameter holes machined between 0.5 and 2 mm from one edge at 0.25 mm increments. Inspection was conducted using an Imasonic (Voray-sur-l'Ognon, France) 128 element ultrasonic array with a nominal centre frequency of 10 MHz and pitch of 0.3 mm, interfaced with a Micropulse FMC model array controller manufactured by Peak NDT Ltd (Derby, UK). The array was gel-coupled to the sample surface closest to the defects and both coherent and diffuse full matrices acquired. Captured windows lengths were 60  $\mu$ s, corresponding to 3000 data points captured at a sampling rate of 50 Mhz. The diffuse full matrix was acquired with a reception delay,  $t_r$ , of 1 ms.

An example of typical time traces, for  $i = j = 64$ , of each full matrix is shown in Fig. 1. It can be seen that the early time signal obscured in the coherent capture has been recovered in the reconstructed data. This preservation of near-surface information is clearer when viewing a larger subset

of the full matrix. Fig. 2 shows the pulse-echo responses for each element ( $i = j$ ), equivalent to a B scan. Here individual near-surface reflections for each hole can easily be discerned in the reconstructed full matrix.

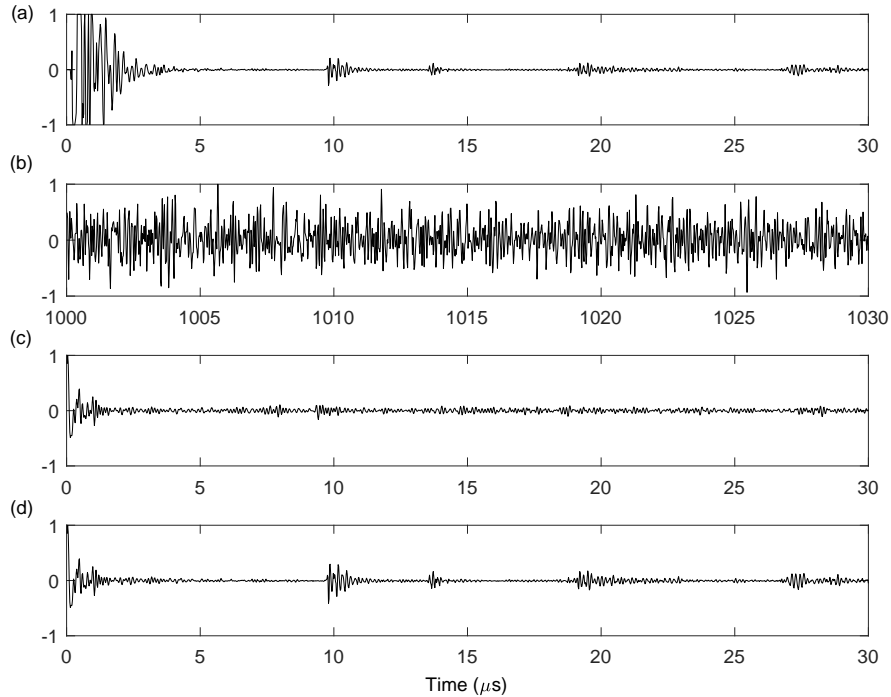


Figure 1: Example time traces for  $i = j = 64$ : (a) coherent full matrix,  $h_{i,j}(t)$ , (b) diffuse full matrix,  $d_{i,j}(t)$ , (c) reconstructed full matrix,  $g_{i,j}(t)$  and (d) hybrid full matrix,  $f_{i,j}(t)$ .

The first back wall reflection, present at approximately  $10 \mu\text{s}$  can be seen in the reconstructed data however not as clearly as when obtained directly. Additionally, the smaller secondary hole reflections are less well resolved in the reconstructed field. As a consequence of the finite number of averaging operations, the recovery of Green's functions within the reconstructed full matrix will always be imperfect and less accurate than directly acquired signals. As such, while near-surface information is obtained more accurately using reconstruction, the response from the interior of the part is better acquired from conventional coherent capture. A more optimal solution is to use early time information from the reconstruction and later time information

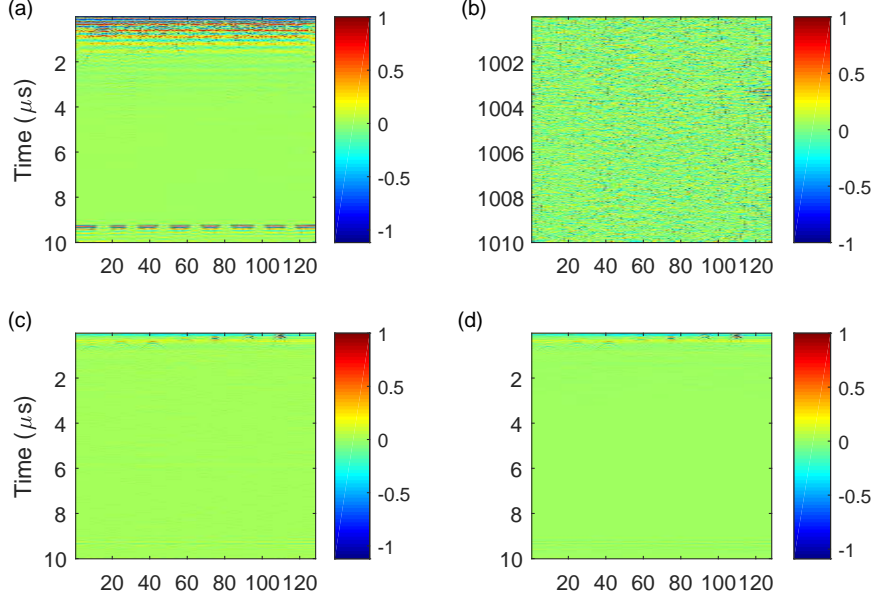


Figure 2: Pulse-echo responses of each element: (a) coherent full matrix,  $h_{i,j}(t)$ , (b) diffuse full matrix,  $d_{i,j}(t)$ , (c) reconstructed full matrix,  $g_{i,j}(t)$  and (d) hybrid full matrix,  $f_{i,j}(t)$ .

from the conventional full matrix. A hybrid full matrix,  $f_{i,j}(t)$ , of the two can be easily obtained by adding the two together with appropriate temporal weighting. One such function is defined as follows in which  $t_c$  denotes the transition time and  $\alpha$  is parameter determining the smoothness of transition

$$f_{i,j}(t) = \frac{1}{1 + e^{-\alpha(t-t_c)}} h_{i,j}(t) + \beta \left( 1 - \frac{1}{1 + e^{-\alpha(t-t_c)}} \right) g_{i,j}(t). \quad (3)$$

The two weighting terms sum to unity, being equal at the time  $t_c$ . Since the relative amplitudes of the coherent and reconstructed matrices are determined by unknown attenuation and dissipation processes, the scaling factor  $\beta$  is required in order to normalise amplitude before summation to form the hybrid matrix. A number of approaches may be taken to the selection of  $\beta$ . One method is to choose a value such that a scattering feature common to both coherent and reconstructed matrices appears with the same amplitude. In this example  $\beta$  is evaluated as the relative amplitude of the first back wall reflection in the coherent and reconstructed matrices. The reflection ampli-

tude is taken as the average value within the pulse-echo responses of each element at the arrival time  $t_b$ . Correspondingly,  $\beta$  is evaluated as

$$\beta = \frac{\sum_{i=1}^N |h_{i,i}(t_b)|}{\sum_{i=1}^N |g_{i,i}(t_b)|}. \quad (4)$$

The responses of the hybrid full matrix for  $\alpha = 25 \times 10^6 \text{ s}^{-1}$ ,  $t_c = 5 \mu\text{s}$  and  $t_b = 9.3 \mu\text{s}$  are shown in Figs. 1(d) and 2(d), from which it can be seen to possess the best signal attributes of the individual full matrices.

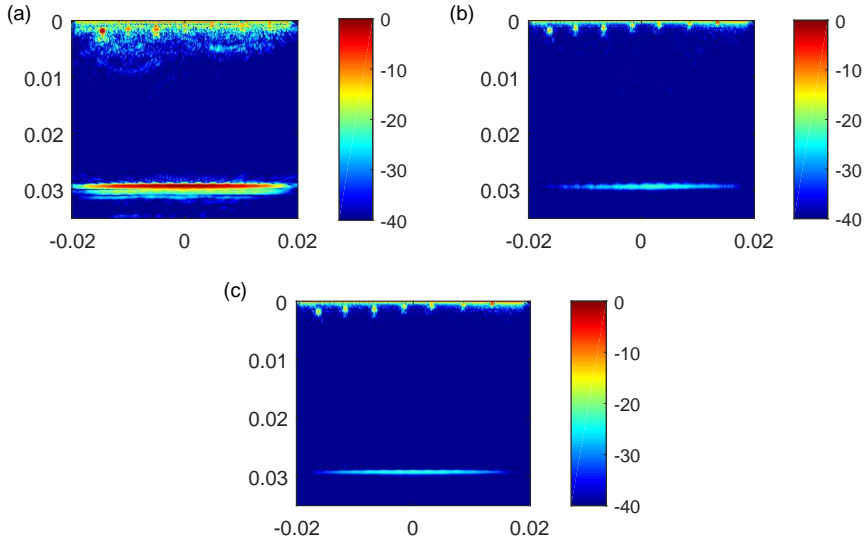


Figure 3: Total focusing method images: (a) coherent full matrix,  $h_{i,j}(t)$ , (b) reconstructed full matrix,  $g_{i,j}(t)$  and (c) hybrid full matrix,  $f_{i,j}(t)$  (Dimensions in mm).

The reconstructed and hybrid full matrices are in a form for which any conventional full matrix imaging technique may be applied without modification. Here images of the specimen are generated using the total focusing method (TFM)[4]. Even though the available near surface information is recovered, the ability to focus in close proximity to the array is still limited as a consequence of element directivity. An aperture limit of  $50^\circ$  is used in



imaging in order to negate this. These TFM images are shown in Fig. 3. As is characteristic of direct contact imaging, the coherent capture image, Fig. 3(a), shows a strong region of artificial noise extending several mm from the array. Although the more distant holes are visible, as the positions move towards the surface they are quickly obscured by the saturation artefacts and become undetectable. Conversely, the image produced from the reconstructed full matrix allows all holes, even within 0.5 mm of the surface, to be resolved with a dynamic range in the order of 30 dB. As would be expected the back wall is however less clear than for the coherent capture. The hybrid full matrix imaging combines the highest quality spatial regions of the other two approaches. This allows both effective near-surface and bulk material imaging from a single directly coupled experimental realisation.

Due to its low acoustic absorption, aluminium is a material well suited to diffuse field measurements. In order to evaluate the applicability of this technique for imaging within more challenging media, the process was repeated on a sample of carbon fibre reinforced polymer (CFRP). The strong scattering and absorption characteristics which make diffuse measurements in composites challenging also necessitate high transmission energy to image deep into a component. This makes the direct contact inspections made possible with this method particularly desirable.

The specimen has dimensions 13x50x20mm and a ply layup of a repeating sequence of 0°, 45°, 90° and 135° orientations. Near surface holes were machined in an identical configuration to the aluminium specimen. Inspection was conducted using a 5 MHz 128 element array with 0.3 mm pitch and, aside from a reduced sampling frequency of 25 MHz, all acquisition parameters were the same as for the previous specimen. The parameters used in the generation of the hybrid matrix were  $\alpha = 50 \times 10^6 \text{ s}^{-1}$ ,  $t_c = 3 \text{ } \mu\text{s}$  and  $t_b = 9.3 \text{ } \mu\text{s}$

TFM images generated using coherent, diffuse and hybrid full matrices are shown in Fig. 4 for an aperture limit of 30° and assumed isotropic velocity of 2900 m/s. As before, in the conventional full matrix image, the near surface is obscured. The remaining image shows coherent backscatter decreasing in amplitude with depth and a weak back wall reflection at 13 mm. Although the precise depth of the holes can not be determined (as a consequence of the longer wavelength), each hole can be individually resolved in the reconstructed full matrix image. Despite the reduced inspection frequency, the diffuse ultrasonic field is of significantly lower amplitude than for the aluminium specimen. A consequence of this is a greater impact of

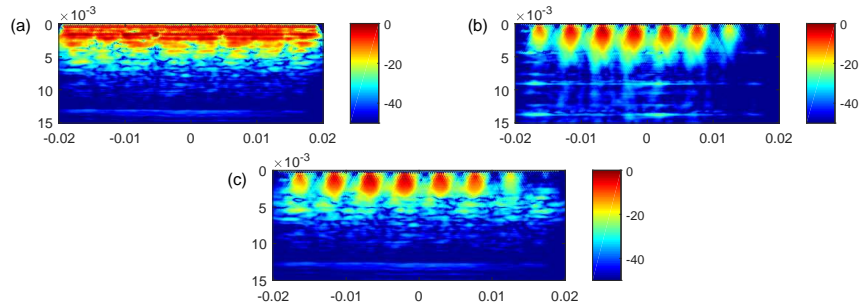


Figure 4: CFRP total focusing method images: (a) coherent full matrix,  $h_{i,j}(t)$ , (b) reconstructed full matrix,  $g_{i,j}(t)$  and (c) hybrid full matrix,  $f_{i,j}(t)$  (Dimensions in mm).

incoherent noise on the reconstructed data. This is evident in Fig. 4(b) for which artefacts caused by period electromagnetic interference can be seen as prominent horizontal lines. In this example the advantage of using a hybrid full matrix is more clearly demonstrated, providing near surface imaging capability but is free of reconstruction artefacts at greater depths.

#### 4. Conclusions

Near surface acoustic information is obscured by nonlinear effects of instrumentation limitations for directly coupled ultrasonic inspections. It is shown here that through cross-correlation of a diffuse full matrix, a reconstructed full matrix can be produced that contains the near-surface information without acquisition artefacts. This process of full matrix reconstruction is demonstrated experimentally on both aluminium and CFRP blocks containing near-surface holes. Whereas many holes are hidden by the region of artificial noise in a conventional coherent capture image, all are easily resolved when using a reconstructed full matrix. It has also shown that combining both coherent and reconstructed full matrices using an appropriate weighting function allows the best properties of both acquisition methods to be exploited, allowing for both near-surface and bulk imaging to be achieved from a single surface coupled measurement.

## References

- [1] Richard L. Weaver and John Burkhardt. Weak anderson localization and enhanced backscatter in reverberation rooms and quantum dots. *The Journal of the Acoustical Society of America*, 96(5):3186–3190, 1994.
- [2] Brnice Froment, Michel Campillo, and Philippe Roux. Reconstructing the Green’s function through iteration of correlations. *Comptes Rendus Geoscience*, 343(89):623 – 632, 2011. Nouveaux dveloppements de limagerie et du suivi temporel partir du bruit sismiqueNew developments on imaging and monitoring with seismic noise.
- [3] Michel Campillo. Phase and correlation in ‘random’ seismic fields and the reconstruction of the Green function. *Pure and applied geophysics*, 163(2-3):475–502, 2006.
- [4] C. Holmes, B. W. Drinkwater, and P. D. Wilcox. Post-processing of the full matrix of ultrasonic transmit-receive array data for non-destructive evaluation. *NDT&E International*, 38:701–711, 2005.
- [5] Eric Larose, Ludovic Margerin, Arnaud Derode, Bart van Tiggelen, Michel Campillo, Nikolai Shapiro, Anne Paul, Laurent Stehly, and Mickael Tanter. Correlation of random wavefields: An interdisciplinary review. *GEOPHYSICS*, 71(4):SI11–SI21, 2006.
- [6] J. N. Potter, A. J. Croxford, and P. D. Wilcox. Nonlinear ultrasonic phased array imaging. *Phys. Rev. Lett.*, 113:144301, Oct 2014.
- [7] Nikolai M. Shapiro, Michel Campillo, Laurent Stehly, and Michael H. Ritzwoller. High-resolution surface-wave tomography from ambient seismic noise. *Science*, 307(5715):1615–1618, 2005.
- [8] Roel Snieder. Extracting the green’s function from the correlation of coda waves: A derivation based on stationary phase. *Phys. Rev. E*, 69:046610, Apr 2004.
- [9] Richard Weaver and Oleg Lobkis. On the emergence of the green’s function in the correlations of a diffuse field: pulse-echo using thermal phonons. *Ultrasonics*, 40(18):435 – 439, 2002.

- [10] Richard L. Weaver and Oleg I. Lobkis. Ultrasonics without a source: Thermal fluctuation correlations at mhz frequencies. *Phys. Rev. Lett.*, 87:134301, Sep 2001.
- [11] Huajian Yao, Robert D. Van Der Hilst, and Maarten V. De Hoop. Surface-wave array tomography in se tibet from ambient seismic noise and two-station analysis i. phase velocity maps. *Geophysical Journal International*, 166(2):732–744, 2006.